SOME APPLICATIONS OF THE CHIRP SONAR

S.G. Schock

Florida Atlantic University
Boca Raton, FL 33431

L.R. LeBlanc

University of Rhode Island
Narrangansett, R.I. 02882

Abstract

A new swept FM, digital subbottom profiler, the chirp sonar, utilizes modern digital signal processing algorithms and hardware (AT&T DSP32C) to generate high resolution images of ocean sediments to 100 meters with 10 cm vertical resolution. Matched-filter processing improves the inband SNR of subbottom returns by at least 20 dB. High SNR allows quantitative analyses such as reflectivity and acoustic attenuation measurements providing surficial and subbottom sediment classification. Reflection profiles showing classified sediments can be used for EEZ, dredging, pipeline, and port and river engineering surveys; geologic studies; and acoustic propagation modeling.

Introduction

The chirp sonar is a towed, digital, swept FM subbottom profiler that generates wideband, quantitative, subbottom reflection data. This quantitative data can be used for generating high resolution images of the water column and/or the underlying sediment structure and for estimating acoustic parameters such as reflectivity, effective attenuation and volume scattering strength of surficial and subfloor sediment layers over a wideband of frequencies. For example, one configuration of the chirp sonar, using a 20 msec 1.5-10 kHz FM sweep, generated images showing a vertical resolution of 15 cm, high spatial resolution(as evidenced by the lack of hyperbole from point scatterers), a subbottom penetration of 62 meters to basement through bay silts and sands, and a dynamic range of 66 dB (measured at the sediment-water interface); and predicted sediment types by calculating the spectrum of subbottom reflections from which the change in acoustic attenuation over the frequency range of the FM sweep was estimated and correlated to sediment type.

High resolution reflection profiles and quantitative measurements, generated by the chirp sonar, are useful for the following applications:

1) geologic, mining, EEZ, port, geotechnical, dredging, environmental impact, deep ocean and hazard surveys requiring wide dynamic range, high resolution images of the seabed and identification of sediment type

2) hydrogeologic surveys requiring porosity and permeability data which can be predicted from attenuation coefficient estimates

3) environmental surveys requiring the detection of thin layers of contaminated sediments or fluidized muds

4) acoustic propagation prediction calculations requiring seabed impedance and acoustic attenuation data

5) water column microstructure studies requiring the spatial variation in the impedance of seawater.

6) sediment gas surveys for mapping the size and spatial distribution of sediment gas bubbles requiring the spectrum of the energy backscattered by the bubbles

7) detecting and imaging buried objects such as archeological artifacts, pipelines and military weapons

8) current scouring surveys requiring a cross sectional image of refilled scour features near bridges, piers and breakwaters

The quantitative chirp sonar was designed and tested at University of Rhode Island under a program sponsored by the Office of Naval Research (Geo-Acoustics/Arctic Sciences Division, Program Manager - Dr. J. Kravitz) to investigate the use of high resolution seismic profilers for remotely measuring sediment properties. The chirp sonar was

developed because the investigation showed that off-the-shelf reflection profilers were not suitable for quantitative analysis (estimation of sediment properties from normal incidence reflection data) due to the following common system problems:
1) poor repeatability of the transmitted acoustic pulse due to the nonlinear behavior of the transducer and/or power supply and/or use of the random seawater/air interface to double the source strength of the projector.
2) projector response which is dependent on submergence pressure
3) source ringing due to transducer resonances and/or lack of control over the transducer excitation voltage transient
4) sonar vehicle motion
5) insufficient signal-to-noise ratios in seismogram data from electronic and acoustic inband noise
6) poor spatial resolution of sonar arrays causing smearing of subbottom features
7) inadequate source and hydrophone baffling causing multipath reception of subbottom images
8) uncalibrated and/or nonlinear electronics preventing reflectivity and attenuation measurements
9) the requirement for a highly trained operator to frequently make amplifier gain adjustments in order to generate a usable seismogram.

During the period of 1985 to 1989, solutions to the above problems were devised and then a prototype, swept FM, quantitative sonar, the chirp sonar, which performed data acquisition and digital signal processing in real time, was designed, constructed and tested at University of Rhode Island (Dept. of Ocean Engineering). A minicomputer with a vector processor and a data acquisition module was required to perform the real time digital signal processing tasks of FM pulse generation, measurement and compression. The prototype sonar sucessfully generated real-time, artifact-free reflection profiles and repeatable, remote estimates of sediment attenuation. The tests of the prototype established the viability of chirp sonar technology, the use of linear, wideband sonar hardware and modern digital signal processing techniques to generate high resolution, quantitative acoustic data[1].

Recent advances in digital signal processing hardware technology allowed the chirp sonar digital signal processing computer to be redesigned around the 80386 Intel microprocessor and the AT&T DSP32C chip, making the system less expensive and more portable. The first microcomputer-based chirp sonar system was manufactured and tested by Datasonics, Inc., Cataumet, Mass. during the first half of 1990 and delivered to Florida Atlantic University where it is being used for sediment classification research.

Chirp Sonar System Description

A block diagram of the microcomputer-based chirp sonar is given in Figure 1. The digital signal processing computer controls the sonar and performs the real-time signal processing functions. A separate chirp pulse computer generates a FM pilot signal for the 2 kW linear power amplifier at a pulse repetition rate determined by the main computer. This pilot signal, which can be swept within the band of .5 to 15 kHz with a duration varying from 5 to 200 msec, contains amplitude and phase compensation, correcting for anomalies in the transmitting and receiving response of the sonar system. These anomalies include transducer resonances which cause source ringing. The power amplifier drives four piezoelectric ceramic piston tranducers which are mounted in a towed vehicle. Subbottom reflections are measured with a ceramic line array which is also mounted within the vehicle. After the output of the array is amplified by a programmable gain amplifier, each return is digitized by a 16 bit A/D converter and processed by the data acquisition computer before it is digitally recorded and displayed as a seismogram on a video monitor and/or a grey scale hardcopy recorder.

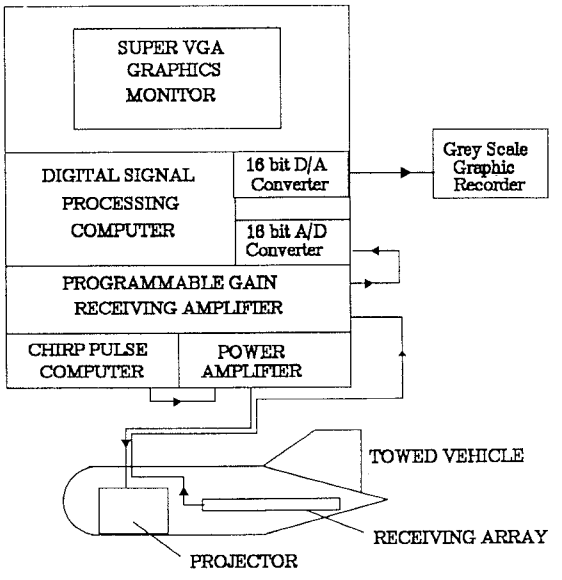

Figure 1. Block diagram of the microcomputer-based chirp sonar

The digital signal processing computer performs the following functions:

1) FM pulse compression using matched-filter processing

2) calculation of the envelope of the compressed signal using a Hilbert transformation

3) spherical spreading and subbottom attenuation corrections to scale envelope data for displaying

4) heave compensation which removes the vertical component of vehicle displacement from the reflection profile

5) sediment/water interface reflectivity calculation and display

6) collection and storage of navigation data

7) control of receiver amplifier gain, pulse repetition rate and A/D conversion delay which are varied automatically as water depth changes

8) dynamic range compression to allow the information contained in the compressed FM data (dynamic range > 66 dB) to be displayed on a video or hardcopy display with limited dynamic range.

The sonar vehicle can be towed as shallow as 1 meter for river surveys to 600 meters for deep ocean surveys. Tow speed can be varied from 0 knots (drifting) for imaging of buried objects to 10 knots for rapid quicklook surveys. Baffling is installed inside the vehicle to reduce direct path transmission between the projector and receiving array and to prevent the reception of downward-traveling multiple reflections off the sea surface or ship's hull.

High Resolution Reflection Profiles

A subbottom profile image (seismogram) is generated by calculating the envelope of each matched-filtered acoustic return, filtering the envelope time series by applying time varying gain (TVG) and dynamic range compression, mapping the amplitude of each sample in the envelope to a color (usually, a shade of gray) and then stacking the arrays of shaded values side-by-side on a display.

To ensure that all subbottom reflections in an acoustic return are displayed in the subbottom profile image, the data must be filtered to compensate for spreading loss, compressional wave attenuation, variations in the amplitude of interface reflections and the limited dynamic range of the video monitor and/or hardcopy printer. The dynamic range of amplitude variations in the envelope for each acoustic return must be reduced to the dynamic range of the display which is commonly 24 dB (for 16 levels of grey or color). Spherical spreading losses can be as high as 40 dB; e.g., when the sonar vehicle is 1 meter above the seafloor and attempting to detect a layer 99 meters beneath the seafloor, the difference between the spreading loss of the seafloor reflection and that of the 100 meter reflection is 40 dB. Losses due to compressional wave attenuation can be much higher; e.g., since the attenuation of a 5 kHz compressional wave traveling through sand (k=0.5 dB/m/kHz) is about 2.5 dB/m, a 12 meter layer of sand will attenuate a reflected wave by 60 dB (based on two way travel). A linear time varying gain (TVG) ramp is applied to the envelope of the return starting at the time of transmission to compensate for spherical spreading. Exponential TVG, starting at the arrival time of the sediment-water interface reflection, corrects for compressional wave attenuation

Even after applying TVG to correct the envelope for spreading and attenuation, the reflection amplitudes within each return can vary by as much as 60 dB depending on the magnitude of the impedance contrast between two adjacent layers, the transmission losses from volume scattering and multi-layer reflection losses, and the thickness of the mixing zone that exists between two adjacent layers. For the case where there is a step change in impedance between two sediment layers, the pressure reflection coefficient can be estimated using

$$R = \frac{\rho_2 c_2 - \rho_1 c_1}{\rho_2 c_2 + \rho_1 c_1} \qquad (1)$$

where ρ and c are the bulk density and complex sound speed of the lossy medium and the subscripts 1 and 2 refer to the medium containing the incident and transmitted waves, respectively.

However, in many cases, the measured pressure reflection coefficient is less than expected because a density gradient exists between sediment layers due to depositional processes and/or vertical mixing of the sediment by erosional and/or biological processes. For example, bioturbation, the mixing of sediments by burrowers, will commonly mix the upper 10 cm of surficial sediments[2,3]. As the surficial layer is buried by a new layer of sediments, the burrowers will mix the two layers thereby generating a transition layer and smearing the impedance contrast between the two layers. Practically, when the vertical width of the transition(mixing) zone between the sediment layers is less than about one-tenth of the acoustic wavelength, the transition can be treated as a step change in impedance.

Because of the existance of density

gradients and the variation in densities between unconsolidated and consolidated material, the measured reflection coefficients can be expected to vary by 40 dB within a typical subbottom return and sometimes as much as 60 dB. For example, consider a thin fluidized mud layer over a hard subfloor such as sand or bedrock. The ratio of the reflection amplitude of the mud-sand interface to that of the water-fluidized mud interface can be as high as 60 dB.

Dynamic range compression is required to reduce the dynamic range of the amplitude fluctuations (>40dB) in the processed return to the range of the display (typically 24 dB). Log compression should be applied to each each envelope so that the noise level of the data is maintained just below the threshold between the first and second gray levels of the display.

To ensure that high quality subbottom images are generated by a reflection profiler, not only must the data be properly scaled as described above, but the following system characteristics are also required: 1) high temporal and spatial resolution 2) baffling to prevent the detection of sea surface reflections 3) transducer ringing suppression and 4) high signal-to-noise ratio of the processed seismogram. The temporal resolution of the compressed FM pulse is approximately equal to the inverse of the effective bandwidth of the sonar system. Since the temporal resolution determines the vertical resolution in a seismogram, a wideband system is necessary. Temporal resolution can be significantly degraded with increasing subbottom depth by compressional wave attenuation. To avoid loss in the vertical resolution with increasing subbottom depth in a subbottom profile, the shape of the transmitted spectrum should be approximately Gaussian.

However, even if the system is wideband, the vertical resolution can be significantly degraded by projector ringing. A ringing source will prevent detection of fine subbottom structure and the detection of a weak reflection following a stronger one. Commonly, the transmitted acoustic pulse is generated by discharging a capacitor into a transducer. This technique of pulse generation causes the transducer to resonate in its most efficient modes, modes that sometimes have low damping causing a series of decaying oscillations in the outgoing pulse. Mechanical damping techniques are difficult to implement due to the high number of poles and zeroes in the response of wideband transducers.

In a linear digital system, electronic ringing suppression is easily implemented by measuring the frequency response of the entire sonar system and then applying an excitation voltage to the transducer correcting for the amplitude and phase anomalies of not only the response of the projector but also that of the receiving array and electronic amplifiers and filters.

Spatial resolution is improved by increasing the aperture of the transmitting and receiving arrays and by the process of matched-filter processing which is used to compress the wideband FM pulses. The matched-filter, designed to attenuate inband noise, also attenuates incoherent energy returned from the frequency dependent spatial sidelobe structure and from off-axis delayed backscattering, and improves the effective spatial resolution of the system.

System noise reduction is performed by the matched filter which is the optimum filter for detecting a known signal in white noise. The inband signal-to-noise improvement realized by a matched filter is given by

$$\Delta SNR = 10\log(T\,BW) \quad dB \qquad (2)$$

where T is the effective pulse length (seconds) and BW is the effective bandwidth of the pulse (Hz). For example, if the chirp sonar transmits a 100 msec pulse with a bandwidth of 10 kHz, the matched filter will improve the inband signal-to-noise ratio of the acoustic return by 30 dB and will remove all out-of-band noise.

An example of a high resolution, wide dynamic range image generated by the chirp sonar is shown in Figure 2. This subbottom profile shows the geologic record of Narragansett Bay since about 18,000 years ago when the last glacier retreated to the north leaving bedrock covered with till. Glacial lake sediments were periodically deposited until 13,000 years ago when erosion breached the southern moraine containing the lake causing the lake to drain. The surface of the lake sediments is uneven because the sediments were eroded by rainfall and dissected by streams. About 7,000 years ago the transgression brought salt water into this area of Narragansett Bay forming marshes and eventually submerging the lake sediments[4]. About 10 meters of bay silts have been deposited above the erosional surface. Note the gas located above one of the organic rich river beds. The image also shows dredged sediments that were dumped on the seafloor. In this profile the bottom multiple appears weak and about as strong as the multiple off the ship's hull (which arrives just before the bottom multiple which is visible beneath the dredge deposits and just above the

buried river bed on the right) because it was redirected by pressure release baffles mounted on the vehicle. These baffles, mounted over the arrays, not only redirected the upward-traveling multiples but also prevented the detection of downward-traveling multiples.

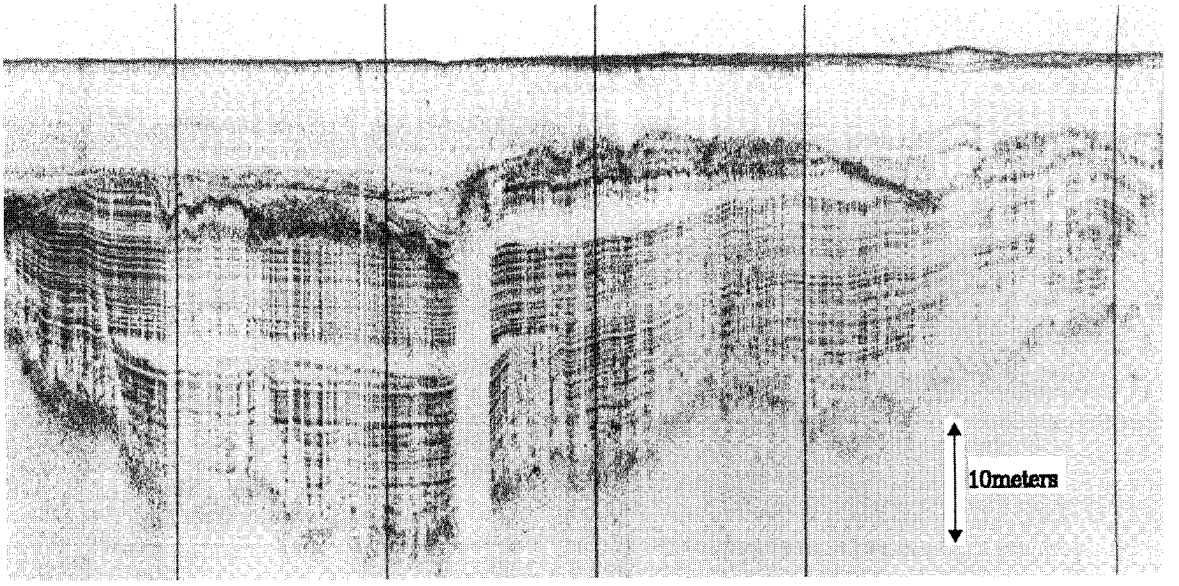

Figure 2. Chirp subbottom profile using a 10 msec 1.8-10 kHz FM sweep. The length of the displayed line is about 1 nautical mile. The tow fish was deployed about 4 meters behind the research vessel and 2 meters beneath the surface. Water depth is about 8 meters. The deepest subfloor penetration, limited by bedrock, is about 40 meters.

The high resolution images can also be used for locating and imaging buried objects. The ability to detect a subbottom target depends on 1) the ratio between the length of the target and distance traveled between chirp transmissions and 2) the ratio of the energy backscattered from the target to the energy of the scattering noise. Both ratios should be kept as large as possible in order to generate the best image of the object. Reducing the horizontal distance between transmissions allows more opportunities for the sonar to detect the target and provides more information for image construction. The horizontal distance between measurements is controlled by changing the pulse repetition rate and/or the ship's speed. The ratio between the energy backscattered from the buried object to that of nearby objects is increased by reducing the height of the sonar off the seafloor which reduces the area of the seabed ensonified by the main lobe and the backscattered noise from scatterers surrounding the object.

An example of the chirp sonar's ability to image buried objects is shown in Figure 3 which shows a decayed log buried beneath the seafloor. Vehicle baffles effectively reduced the amplitude of the water multiples which would have created a significant amount of interference in this very shallow area which has a relatively hard seafloor of silty sands and shells. Note the high spatial resolution of the chirp allows accurate delineation of the shape of the log without the characteristic hyperbolas at the ends of the log.

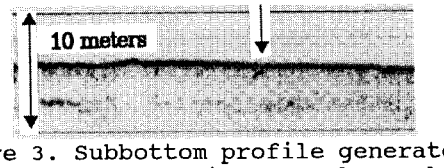

Figure 3. Subbottom profile generated by chirp sonar showing a decayed log detected beneath a silty sand in 2.5 meters of water. The chirp sonar utilized a 10 msec 1.8-10 kHz FM sweep to generate this image. The fish was towed at a depth of 1.5 meters and at a estimated speed of 0.3 m/s. The diver who recovered the log visually estimated that the upper end of the log was about 15 cm beneath the seafloor and the lower end was about 50 cm beneath the floor. The log was 10 cm in diameter and 1.5 meters long.

Quantitative Measurements

The chirp sonar estimates two parameters which can be used to classify sediments: the pressure reflection coefficient and the effective attenuation coefficient both of which are estimated

by analyzing an interface reflection.

The pressure reflection coefficient, the ratio of the pressure amplitude of a reflected wave to that of an incident wave, can be used to classify the surficial sediment layer either by directly correlating the coefficient with sediment type, or calculating the impedance of the surficial sediment layer using equation(1) and correlating the impedance with the sediment type.

Since the complex sound speed **c** is approximately frequency independent over one decade for ocean sediments, equation (1) indicates that the measured reflection coefficient should be independent of frequency. However, it is common to find that the measured reflection coefficient is dependent on frequency. This dependence occurs when an impedance gradient exists at the sediment-water interface and is caused by interfering reflections that are generated by the sequence of small, closely spaced impedance changes that make up that gradient. Spectral analysis of the sediment water interface reflection can be used to determine the frequency dependence of the reflection coefficient and the accuracy of the reflectivity measurement.

Subsurface sediment layers can be classified by calculating the impedance of each layer and correlating the impedance with sediment type or physical sediment properties. Several methods exist for recovering acoustic impedance from band-limited acoustic profiles[5]. Statistical techniques have been used to study the relationships between acoustic impedance and physical properties[6]. Impedance can be used to predict bulk density for a specific depositional area when the relationships between the bulk density and sound speed are known[7].

The effective attenuation coefficient can also be used to classify sediments and to estimate physical sediment properties.

The attenuation of a wideband pulse traveling through a lossy medium can be described in terms of the pressure amplitude spectrum:

$$A(f,x)=A(f,0)10^{-\frac{a(f)}{20}x} \qquad (3)$$

where attenuation a(f) in (dB/m) is commonly expressed as

$$a(f)=k(\frac{f}{1000})^{n} \qquad (4)$$

where k is the attenuation coefficient (dB/m/kHz), x is the distance that the wave traveled, and A(f,0) is spectrum of the pulse at position x=0.

The procedure for estimating the attenuation coefficient can be seen if we solve (3) for a(f) and assume n=1:

$$a(f) = -\frac{1}{x}20\log[A(f,x)/A(f,0)] \qquad (5)$$

To estimate the attenuation coefficient from a subbottom reflection, let x be the two way distance (estimated based on an assumed wave speed) that the pulse traveled through the sediment , and plot a(f) vs. f/1000 (kHz). The slope of the least squares line fitted through the plotted data is the estimated attenuation coefficient k. A close fit indicates that the assumption of the linear variation of attenuation with frequency(n=1) was valid.

This measurement does not require knowledge of geometric transmission losses but only the shape of the amplitude spectra of the unattenuated pulse and the attenuated pulse. Geometric transmission losses and other frequency independent errors will change the intercept of the a(f) vs f curve but not the slope, the estimated attenuation coefficient k. Since a(0) is unknown, the estimated coefficient k can not be directly used to calculate the absolute attenuation a(f) (dB/m) at a particular frequency by multiplying k by f.

The attenuation coefficient, which is related to several physical sediment properties, can be used for sediment classification. Relationships between the attenuation coefficient k and porosity,permeability and mean grain size and other physical properties have been established by experiment and by modeling[8,9].

The spectra of the volume scatters can be used for sediment gas studies. The magnitude and the resonances of the backscattered spectra can be used to estimate the sediment gas concentration and bubble size. Expressions describing the acoustics of gassy sediments including bubble dynamics and compressional wave attenuation have been developed and verified by laboratory experiments[10].

Conclusions

The chirp sonar is the most versatile and capable subbottom profiler available today. It was designed by applying digital FM signal processing and linear systems analysis techniques to highly linear, wideband sonar hardware. Projector ringing suppression, high SNR(>60dB), high temporal and spatial resolution are some of the features of

the chirp sonar that enable it to generate subbottom profiles showing the fine structure of the seabed without any significant loss in resolution with subbottom depth.

Additionally, the wide dynamic range acoustic returns can be used to spectrally analyze subbottom reflections and volume scattering. These measurements can be for estimating acoustic attenuation, reflectivity and the resonances of volume scatterers providing the inputs for acoustic propagation and sediment classification models and sediment gas studies.

References

1. S.G. Schock, L.R. LeBlanc, and L.A. Mayer, "Chirp subbottom profiler for quantitative sediment analysis," Geophysics **54**, 445-450, 1989.

2. N.L. Guinasso and D.R. Schink, " Quantitative estimates of biological mixing rates in abyssal sediments," J. Geophy. Res. **80**, 3032-3043, 1975.

3. M.L. Richardson, D.K. Young, and K.B. Briggs, "Effects of hydrodynamic and biological processes on sediment geoacoustic properties in Long Island Sound, U.S.A.," Mar. Geol. **52**, 220- 226, 1983.

4. R.L. McMaster, "Holocene Stratigraphy and Depositional History of the Narragansett Bay System, Rhode Island," Sedimentology **31**, 777-792, 1984.

5. D.W. Oldenburg, T. Scheuer, and S. Levy, "Recovery of the acoustic impedance from reflection seismograms," Geophysics **48**, 1318-1337, 1983.

6. R.T. Bachman, "Acoustic and physical property relationships in marine sediment," J. Acoust. Soc. of Amer. **78**, 616-621, 1985.

7. E.L. Hamilton, "Geoacoustic modeling of the seafloor," J. Acoust. Soc. Amer. **68**, 1313-1340, 1980.

8. E.L. Hamilton, "Compressional-wave attenuation in marine sediments," Geophysics **37**, 620-646, 1972.

9. A. Turgut and T. Yamamoto, "Synthetic seismograms for marine sediments and determination of porosity and permeability," Geophysics **53**, 1056-1067, 1988.

10. A.L. Anderson and L.D. Hampton, "Acoustics of gas-bearing sediments. II. Measurements and models," J. Acoust. Soc of Amer. **67**, 1890-1903, 1980.